Changes in Human Meibum Lipid Composition with Age Using Nuclear Magnetic Resonance Spectroscopy

Douglas Borchman,[1] Gary N. Foulks,[2] Marta C. Yappert,[3] and Sarah E. Milliner[3]

PURPOSE. Human tear film stability decreases with increasing age. In this study, the changes in meibum composition were measured in search of markers of tear film instability.

METHODS. ^{1}H NMR nuclear magnetic resonance (NMR) spectra of 43 normal donors aged 1 to 88 years were acquired.

RESULTS. Compared with meibum from adolescents and adults, meibum from infants and children contains less CH_3 and $C=C$ groups and an increased aldehyde-to-lipid hydroperoxide ratio.

CONCLUSIONS. It is reasonable that tear film stability is higher in infants than in adults. Their meibum contains less CH_3 and $C=C$ groups and higher levels of protein, and as a result, the lipid is more ordered because of the tighter and stronger lipid–lipid interactions. For water to evaporate, it must first pass through the tight lipid–lipid barrier. For tears to break up, lipid–lipid interactions must be broken. It is reasonable that because the lipid–lipid interactions are stronger in infants' and children's tears compared with those of adolescents and adults, the tear film in the younger groups is more stable and provides a better barrier to evaporation than does the tear film of adults. Lipid saturation could be the critical feature in meibum that stabilizes tears in infants. (*Invest Ophthalmol Vis Sci.* 2012;53:475–482) DOI:10.1167/iovs.11-8341

Tears of infants are much more stable than those of adults.[1-15] As we age, the rate at which we spontaneously blink increases from less than one time a minute in infants to as much as 20 times per minute in adults. (See Fig. 5 in Ref. 15.) Tear break-up time is related to the spontaneous blink rate and decreases from as high as 35 seconds in infants to 8 to 16 seconds in adults[2,6-8] and is below 5 seconds in adults with meibomian gland dysfunction (MGD).[16-19] By understanding how tear film instability, meibum delivery, and lipid composition are affected by age, sex, and race in normal donors, we can gain insight into the biomarkers responsible for tear film instability in MGD.

Aside from a few spectroscopic studies discussed below, there have been no studies to determine age-related changes in meibum composition or conformation. Infrared and Raman spectroscopy show that meibum from children has fewer CH_3 groups, double bonds, and cholesterol esters and less protein[20] and more carotenoids[21] than does that from older normal adults and adults with MGD. Five conformational/environmental biomarkers have been found that may also be related to tear film instability. Conformation is the secondary structural arrangement of the molecules in space and may be critical to tear film function. The carbonyl moieties in meibum from young donors with a more stable tear film are in an environment with a stronger dielectric constant (an environmental biomarker),[22] and the hydrocarbon chains are more ordered (a conformational biomarker)[20,23] (more *trans* rotomers), with stronger lipid–lipid interactions (a conformational biomarker)[23] and a higher phase transition temperature (a conformational biomarker)[20,23] than in adults without dry eye syndrome. Temperature-induced phase transitions of meibum lipid were experimentally reproducible and similar in multiple samples collected from the same person.[24] At ambient lid temperature, the lipid is approximately 37% ordered, between a solid (gel phase) and a liquid (liquid crystalline phase).[25] As the temperature increased from 25°C to 45°C, lipid delivery to the margins was observed to increase, with a concomitant decrease in the refractive index,[26] hydrocarbon disorder,[24] and meibum lipid hydrocarbon motion.[25] These findings suggest that hydrocarbon chain order and motion could determine the delivery of meibum lipid from the meibomian glands to the lid margins and subsequently to the tear film.[20,27]

Meibum from normal donors (Mn) is approximately 40% less ordered at 33.5°C compared with lipid extracted from tears, indicating that tears do not have the same lipid composition as Mn.[24] For Mn and other tissues, lipid saturation and lipid order at a physiological temperature were linearly related to the lipid phase-transition temperature.[21] Mn from normal donors ranging in age from 3 to 88 years of age was studied.[22,28] Mn phase transitions were quantified by fitting them to a four-parameter, two-state sigmoid equation. Mn order and phase-transition temperatures decrease with age, and this trend may be attributable to lipid compositional changes.[22,28]

Infrared and Raman spectroscopy have been applied to the study of meibum hydrocarbon chain conformation and have provided limited information regarding meibum composition.[21,24,28-30] These techniques may be applicable to high-throughput screening, and FTIR has recently been used as a diagnostic tool.[20] The advantage of spectroscopic techniques is that the sample is not destroyed in the process of analysis and the same sample can later be analyzed by other techniques, including mass spectrometry. Nuclear magnetic resonance (NMR) spectroscopy has been useful for discovering and characterizing new lipids in the human lens[31-36] and in quantifying waxes, the primary structure, and the composition of the cholesterol esters and triglycerides that are major components of human meibum.[37-47] We used NMR to quantify the relative

amount of wax, cholesterol esters, and glycerides in meibum from donors, with or without MGD.[48] The intensity, width, and frequency of bands measured in our infrared and Raman spectroscopic studies of meibum are often sensitive to the environment, and conformational variations about the moieties associated with the band complicate compositional analysis. Unlike vibrational and electronic spectroscopy and if aggregation does not occur, the area of ^{1}H-NMR resonances is proportional to the number of protons and is not affected by the surrounding environment. Therefore, quantitative studies based on ^{1}H-NMR do not require standards for every different chain length and saturation. In this study, we used NMR spectroscopy to quantify changes in meibum composition with age.

MATERIALS AND METHODS

The protocols used have been published and are quoted below.[48]

Materials

Cyclohexane-d_{12}, tetrahydrofuran (THF), tetramethylsilane (TMS), and methanol (MeOH) were obtained from Sigma-Aldrich (St. Louis, MO).

Clinical Diagnosis

The subjects were recruited from the Kentucky Lion's Eye Center and the Robley Rex Veterans Affairs Medical Center (Louisville KY). Normal status was assigned when the subject's meibomian gland orifices showed no evidence of keratinization or plugging with turbid or thickened secretions, and no dilated blood vessels were observed on the eyelid margin.

Collection and Processing of Human Meibum

Written, informed consent was obtained from all donors. Protocols and procedures were reviewed by the University of Louisville Institutional Review Board and the Robley Rex Veterans Affairs Institutional Review Board. All procedures were in accord with the Declaration of Helsinki. Meibomian glands were expressed by compressing the eyelid between cotton-tipped applicators with strict attention to avoid touching the eyelid margin during expression. All four eyelids were expressed, and approximately 1 mg of meibum (ML) was collected per individual for direct spectroscopic study. The expressate was collected with a platinum spatula and immediately spread onto an AgCl window and into 0.5 mL of THF/MEOH (3:1 vol:vol) in a 9-mm microvial with a Teflon cap (Microliter Analytical Supplies Ind., Suwanee, GA). Argon gas was bubbled onto the samples to prevent oxidation. The sample on the AgCl window and in the vial were capped and frozen under argon gas until analysis. Analyses were performed within 3 weeks of collection of the sample. Storage of the sample on AgCl windows for over 2 months under argon did not affect the sample.[21] Before NMR analysis, the THF/MeOH in the microvial containing ML, rinsed from the spatula as described above, was evaporated with a stream of argon gas.

After infrared analysis and solvent evaporation, ML was removed from the AgCl window by using a series of solvents with different hydrophobicities, to ensure that all lipid classes were extracted from the window. First, the AgCl window was placed with the ML side down into a 15-mL glass scintillation vial containing 1 mL of hexane

and purged with argon gas to avoid oxidation. A glass vial, rather than a plastic one, was used in all protocols to avoid plasticizer contamination. The vial was sonicated in an ultrasonic bath (model 1510; Branson Ultrasonics, Danbury, CT) for 10 minutes. The hexane was decanted into the microvial containing the ML rinsed from the spatula. The hexane was evaporated under a stream of nitrogen gas. Methanol (1.5 mL) was then added to the scintillation vial containing the AgCl window and purged with argon gas. The vial was sonicated in an ultrasonic bath (Branson Ultrasonics) for 10 minutes. The methanol was decanted into the microvial containing the ML rinsed from the spatula and was evaporated under a stream of nitrogen gas. THF/MeOH (1.5 mL) was added to the scintillation vial containing the AgCl window and purged with argon gas. The vial was sonicated in an ultrasonic bath (Branson Ultrasonics) for 10 minutes. The microvial containing the extracted meibum lipid was lyophilized for 12 hours to remove trace amounts of organic solvents. Finally, deuterated cyclohexane (0.5 mL), with a small amount of tetramethylsilane for a reference band, was added to the sample and sonicated (Branson Ultrasonics) for 10 minutes in a bath sonicator. The solution was transferred to glass NMR tubes (Sigma-Aldrich) and NMR spectra were collected.

NMR Spectral Measurements

Spectral data were acquired (Inova-500 spectrometer; Varian, Lexington, MA), with the following parameters: Eight hundred scans were acquired with a spectral width of 15 ppm, 60° pulse, 4-K data points, 1.0-second delay time, and 2.049-second acquisition time at 25°C. The TMS resonance was set to 0 ppm. Commercial software (GRAMS 386; Galactic Industries Corp., Salem, NH) was used for spectral deconvolution and curve fitting. The area of each band was used for the quantification of lipid composition.

Statistics

Data are presented as the average ± SEM. Statistical significance was determined with Student's *t*-test or the correlation coefficient from the linear regression best fit. Differences reaching $P < 0.05$ were significant.

RESULTS

NMR spectra of meibum from 43 normal donors without dry eye symptoms were measured. Spectra were initially grouped by age according to Table 1. We found no significant differences in the relative intensities of most of the resonances between the child, adolescent, and adult groups. Therefore, and for simplicity, data from these groups were combined except when discussed in the section on Resonances that Change between the Child and Adolescent Groups.

A typical ^{1}H NMR spectra of human meibum (Fig. 1) may be divided into five regions: the CH_2 and CH_3 region from 0 to 1.4 ppm, the CH and deshielded CH_2 region from 1.4 to 3.9 ppm, the ester region from 3.9 to 4.7, the C=C region from 4.7 to 7 ppm, and the oxidative products region above 7 ppm. Tentative band assignments were made from ^{1}H and ^{13}C NMR studies of waxes and triglycerides, oils and waxes (Table 2).[37–48] Five

TABLE 1. Meibum Donor Grouping and Characteristics

	Average Age (y)	Age Range (y)	Male (%)	Race (%)	Number Sampled
Infant	1.1	<1–2	86	C (57), B (14), H (14), U (14)	7
Child	7.6	3–12	57	C (100)	7
Adolescent	23	13–32	71	C (59), A (41)	17
Adult	65	52–88	92	C (84), B (8), A (8)	12

C, Caucasian; B, Black; H, Hispanic; U, unknown.
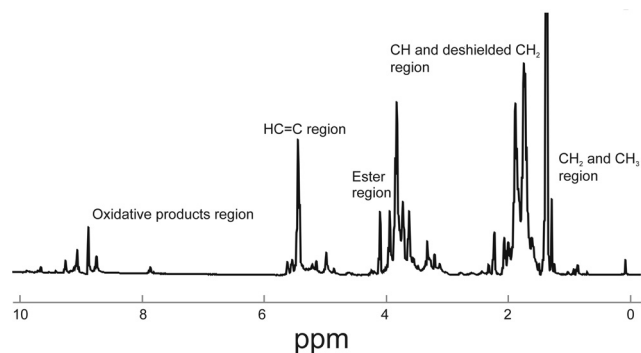
FIGURE 1. An average ^{1}H NMR spectrum of human meibum from donors with meibomian gland dysfunction. The ^{1}H NMR spectra of human meibum may be divided into five regions: the CH_2 and CH_3 region from 0 to 1.4 ppm, the CH and deshielded CH_2 region from 1.4 to 3.9 ppm, the ester region from 3.9 to 4.7, the C=C region from 4.7 to 7 ppm, and the oxidative products region above 7 ppm.

bands, discussed below, changed significantly ($P < 0.05$, between the infant/child and adult groups; Table 2, Fig. 2).

The CH_2 and CH_3 Region

The resonance at 1.39 ppm is the most intense and corresponds to the $—(CH_2)_n—$ protons (Fig. 1). The area of this resonance relative to the total area of all the resonances did not change significantly in the child, adolescent, or adult groups; however, the ratio was significantly higher ($P < 0.05$) in the infant group compared with the average ratios in the other groups (Fig. 2D).

The CH_3 ^{1}H NMR resonance region of a typical NMR spectrum of human meibum is shown in Figure 3. C**H**$_3$ protons (the proton moiety associated with the resonance is underscored in the text, figures, and tables) excluding methylene moieties near omega 3 double bonds are seen near 0.89 ppm (Fig. 3). Methylene moieties near omega 3 double bonds form a triplet centered near 0.94 ppm (Fig. 3). The resonance at 1.03 ppm (Fig. 3) has been tentatively assigned to the $—CH_2OHCH_2$ C**H**$_3$

and $—CH_2—C\underline{H}—$ $(CH_3)_2$ isobranched protons. The assignments for the proton resonances near 1.29 and 1.26 ppm are less certain and have tentatively been assigned to methylene protons associated with short chain esters (Fig. 3, Table 2). Two proton resonances near 0.72 and 0.09 ppm appear in all the NMR spectra of human meibum and are relatively less intense, only a thousandth of the intensity of the 1.39 CH_2 resonance (Table 2, resonance not shown). No proton assignments were made for these resonances.

The areas of the three CH_3 resonances at 0.89, 1.03, and 1.29 ppm increased with age relative to both the area of total protons (Figs. 2A–C) and relative to the area of the major CH_2 resonance at 1.39 ppm (Table 2). To confirm the changes in the area ratios of the various resonances versus the resonance at 1.39 ppm and the total protons, area ratios were calculated relative to the area of the resonance of wax ester protons at 4.1 ppm. The areas of the three CH_3 resonances at 0.89, 1.03, and 1.29 ppm relative to the area of the 4.1-ppm resonance were significantly higher in the infant group relative to the other groups ($P = 0.031$, 0.042, and 0.044, respectively). The areas of the resonances at 0.89, 1.03, and 1.29 ppm relative to the areas of the resonances at 1.39 and 4.1 ppm and the total of the resonances confirm that the infant group had relatively more CH_3 moieties than did the other groups.

It should also be noted that the resonance at 0.94 ppm was significantly ($P = 0.02$; >300%) higher in the infant group than in the other groups when compared with the area of the 4.1-ppm wax ester resonance.

The validity of our CH_2 and CH_3 area measurements was tested by analyzing the ^{1}H-NMR spectra of eight different waxes spanning a wide range of chain lengths and saturation: steryl oleate, oleyl oleate, palmityl oleate, arachidyl oleate, steryl sterate, palmityl palmitate, myristyl aurate, and palmityl laurate. As expected, the ratios of the areas of the resonances at 3.98 and 0.88 ppm, assigned to the two protons of the first CH_2 group in the alkyl chain of the waxes and to the six protons of the two-terminal CH_3, respectively, were not dependent on saturation or chain length and averaged 0.322 with an SD of 0.008. This result is close to the expected ratio of 0.333 (two to six protons). Palmityl laurate contains the short-

TABLE 2. Integrated Band Intensities Relative to 1.39 CH_2 Resonance

Chemical Shifts (ppm)	Infant	Child-Adult	*P*	Tentative Assignment
0.09	0.00061 ± 0.00003*			No assignment
0.72	0.00044 ± 0.00014	0.00151 ± 0.00022		No assignment
0.89	0.0077 ± 0.0019	0.0209 ± 0.0028	0.049†	$-C\underline{H}_3$, except n-3
0.94	0.0015 ± 0.0003	0.0033 ± 0.0013	0.14	$-C\underline{H}_3$, n-3
1.03	0.00030 ± 0.00014	0.0014 ± 0.0002	0.023†	$-CH_2OHCH_2$ C$\underline{H}_3$
				$-CH_2-C\underline{H}-(CH_3)_2$, isobranched
1.26	0.0047 ± 0.0002	0.0041 ± 0.0002	0.19	$-COO(CH_2)nC\underline{H}_3$, short-chain esters
1.29	0.014 ± 0.0053	0.058 ± 0.009	0.024†	$-COO(CH_2)nC\underline{H}_3$, short-chain esters
1.39	1	1	1	$-(C\underline{H}_2)_n-$, Core,
1.70	0.43 ± 0.04	0.43 ± 0.04	1	$R-C\underline{H}_2-CH_2-COO-R$
4.10	0.036 ± 0.003	0.026 ± 0.003	0.2	$ROC\underline{H}_2$-alkyl, wax ester
4.18	0.0047 ± 0.001	0.0031 ± 0.0005	0.2	$CHC\underline{H}_2OR$; C1,3 protons, glyceryl. 4 H per molecule
4.25	0.0033 ± 0.0004	0.0036 ± 0.0004	0.7	C1,3 protons, glyceryl
4.6	0.0047 ± 0.0002	0.0047 ± 0.0008	1	$R-O-C\underline{H}$, C3 of cholesterol ester
4.85	0.000415 ± 0.000051	0.0114 ± 0.0040	0.23	$-C\underline{H}=C\underline{H}-$, conjugated
5.0	0.015 ± 0.0011	0.042 ± 0.0083	0.135	$-C\underline{H}=C\underline{H}-$, conjugated
5.2	0.012 ± 0.008	0.033 ± 0.0068	0.17	$-C\underline{H}=C\underline{H}-$, conjugated
5.45	0.115 ± 0.02	0.206 ± 0.012	0.0019†	$-C\underline{H}=C\underline{H}-$
7.9	0.0051 ± 0.0001	0.0087 ± 0.0013	0.25	Hydroperoxides
8.7	0.072 ± 0.014	0.108 ± 0.012	0.17	
9.65	0.0011 ± 0.00018	0.0020 ± 0.0008	0.63	*trans*-2-alkenals
9.71	0.00017 ± 0.00002	0.00026 ± 0.00004	0.17	$R-C\underline{H}=O$, *n*-alkenals

* Average of all samples.
† Significant difference.
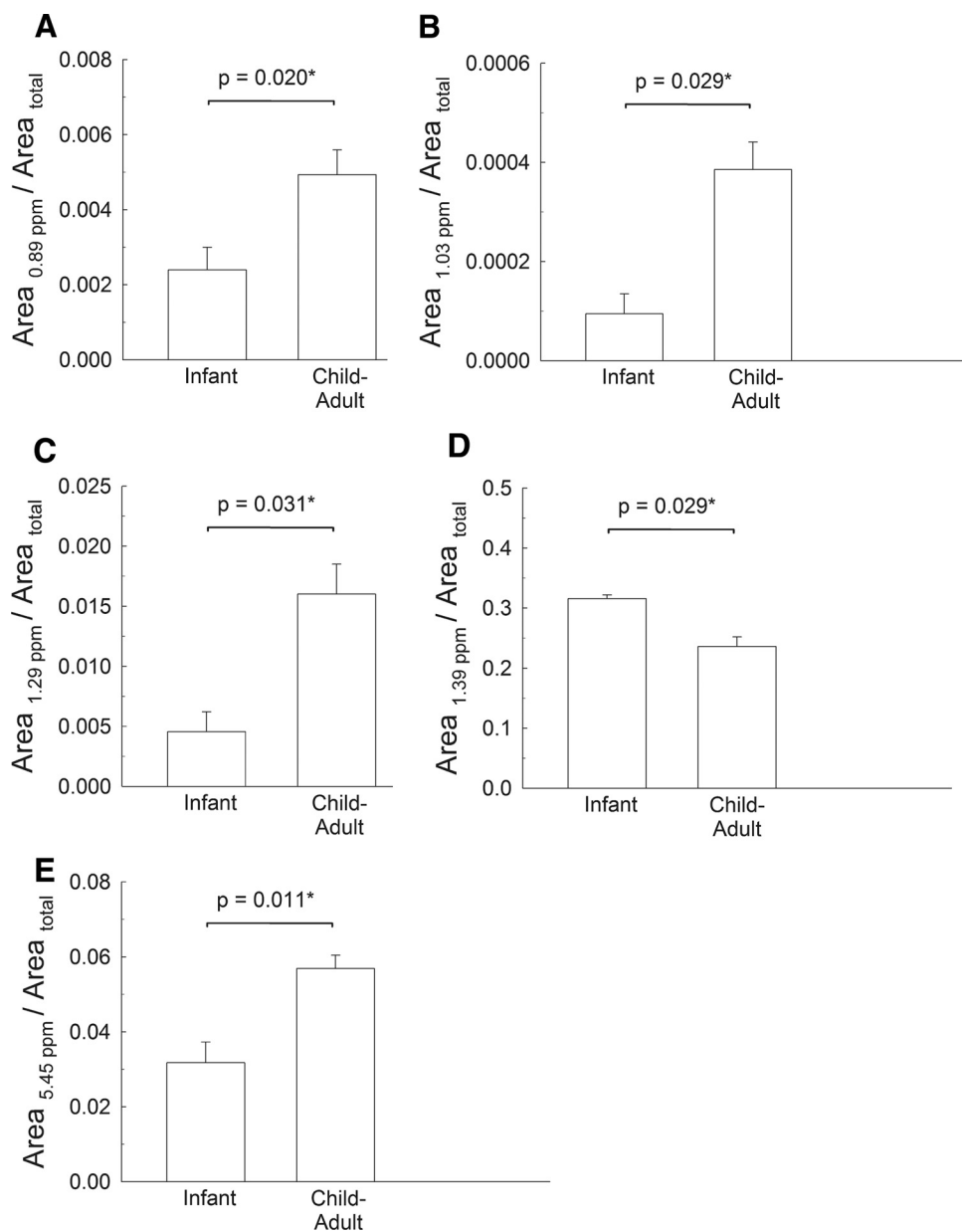
FIGURE 2. The relative areas of bands that changed between the infant group and child-adult groups. Area total is the total area for all the proton resonances. Resonance assignments are given in Table 2. Sample data are provided in Table 1.

est alkyl chain length (12 carbons) whereas arachidyl oleate has the longest alkyl chain (20 carbons). The ratios were 0.328 and 0.327, the shortest and longest alkyl chain waxes, respectively. This exemplifies one of the advantages of ^{1}H-NMR over mass spectrometric analysis: The area of ^{1}H-NMR resonances is proportional to the number of protons and is not affected by the surrounding environment. Therefore, quantitative studies based on ^{1}H-NMR do not require standards for every different chain length and saturation, as do mass spectrometric methods.

Double-Bond Region

Proton resonances associated with C=C bonds are located between 4.8 and 6 ppm (Fig. 1). One of the most intense proton resonances in the ^{1}H NMR spectra of human meibum appears at 5.45 ppm and is assigned to *cis* C=C bonds (Fig. 1, Table 2). Three proton resonances associated with conjugated double bonds appear near 5.2, 5.0, and 4.87 ppm (Fig. 1, Table 2). The resonance near 5 ppm has been assigned to squalene.[47] Compared with infants, the averages

of the relative areas of all the signals in the C=C region were higher (Table 2, $P < 0.05$) in the averages of the children, adolescent, and adult groups. The relative area of the resonance at 5.45 increased significantly ($P < 0.05$) in the child to adult groups compared with that of the infant group when compared with the area of the resonance at 1.39 ppm (Table 2) and the area of the total proton resonances (Fig. 2E). The area of the resonance at 5.45 relative to the area of the 4.1-ppm resonance was also significantly ($P = 0.011$; >300%) higher in the infant group relative to the other groups. It is reasonable to conclude that as the number of double bonds increases with age (Fig. 2E), the number of CH_2 moieties per total protons decreases (Fig. 2D).

A standard curve was prepared from measurements of mixtures of the two waxes, palmityl palmitate and oleyl oleate, ranging from 2 HC=CH moieties per hydrocarbon chain to 0 (Fig. 4A). As a measure of saturation, the ratio of the area of the *cis* CH=CH resonance near 5.45 ppm was divided by the area of the CH_2 resonance for protons next to
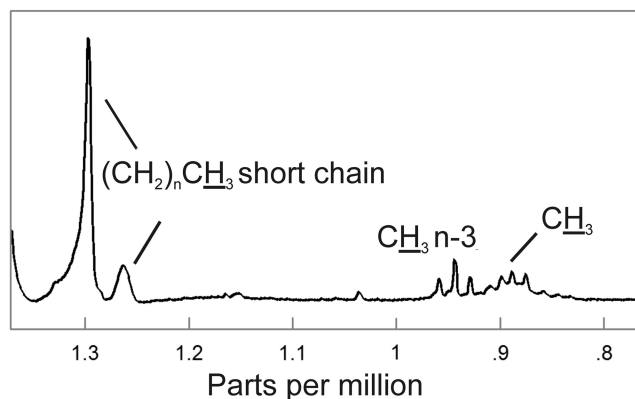
FIGURE 3. ^{1}H NMR spectrum of meibum from a 4-year-old Caucasian girl. The region contains protons assigned to CH$_3$ moieties. The proton moiety associated with the resonance is underscored.

the ester bond at 3.98 ppm (Fig. 4B). The standard curve was linear ($r = 0.9989$), with a slope of 2.06 ± 0.02. The slope was near the expected value of 2. The correlation coefficient close to 1 indicates that the experimental error is small relative to the much larger standard errors obtained from meibum sample to meibum sample in Figures 2 and 5 and Tables 2 and 3.

Resonances that Change between the Child and Adolescent Groups

The relative areas of four resonances were found to change between the child and adolescent groups. These resonances are shown in Figure 5 and Table 3. Note that the changes were significant ($P < 0.05$) when the resonances were divided by the area of total protons (Fig. 5) or the area of the resonances at 1.39 and 4.1 ppm (Table 3).

Oxidative Products Region

Products of lipid oxidation appear from 5.5 to 10 ppm.[49,50] Four proton resonances were observed at 7.9, 8.7, 9.65, and 9.71 ppm in all the human meibum ^{1}H NMR spectra (Fig. 1, Table 2). The resonances between 6 and 9 ppm were assigned to hydroperoxides and those between 9 and 10 were assigned to aldehydes (Table 2). The average areas of all the resonances due to lipid oxidation relative to the area of the 1.39 ppm signal were higher in the children, adolescents, and adults than in the infants, but the comparison was not statistically significant ($P > 0.05$; Table 2). When the area of the two aldehyde resonances were added together and divided by the area of the two hydroperoxide resonances, the ratio increased significantly ($P < 0.05$) with age (Fig. 6). Since the ratio of aldehydes to hydroperoxides was larger in the older group, the breakdown of hydroperoxides was greater in the older group than in the younger one.
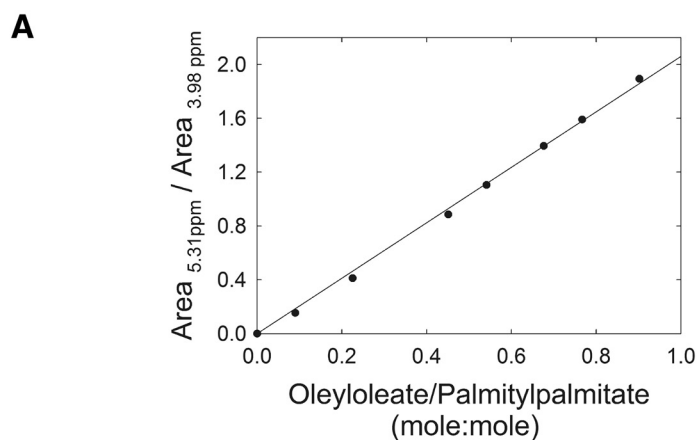

FIGURE 4. (A) A standard curve was prepared from the ^{1}H NMR spectra of mixtures of palmityl palmitate and oleyl oleate, using the area ratio of the resonances at 3.98 and 5.31 ppm to determine hydrocarbon chain saturation. The standard curve was linear ($r = 0.999$), with a slope of 2.06 ± 0.02. (B) Some of the ^{1}H NMR spectra of mixtures of palmityl palmitate and oleyl oleate used to make the standard curve in (A). Proton resonances associated with the ester protons next to the ester bond of wax appear at 3.98 ppm. Proton resonances associated with HC=CH bonds are located at 5.31. The lowest intensity in the 5.31-ppm resonance region is due to palmityl palmitate with no double bonds. The highest intensity in the 5.31-ppm resonance is due to oleyl oleate, with two double bonds per molecule. Between these spectra at 5.31 ppm are spectra of palmityl palmitate/oleyl oleate at 0.25 and 0.6 (wt:wt).

A

B

C

D
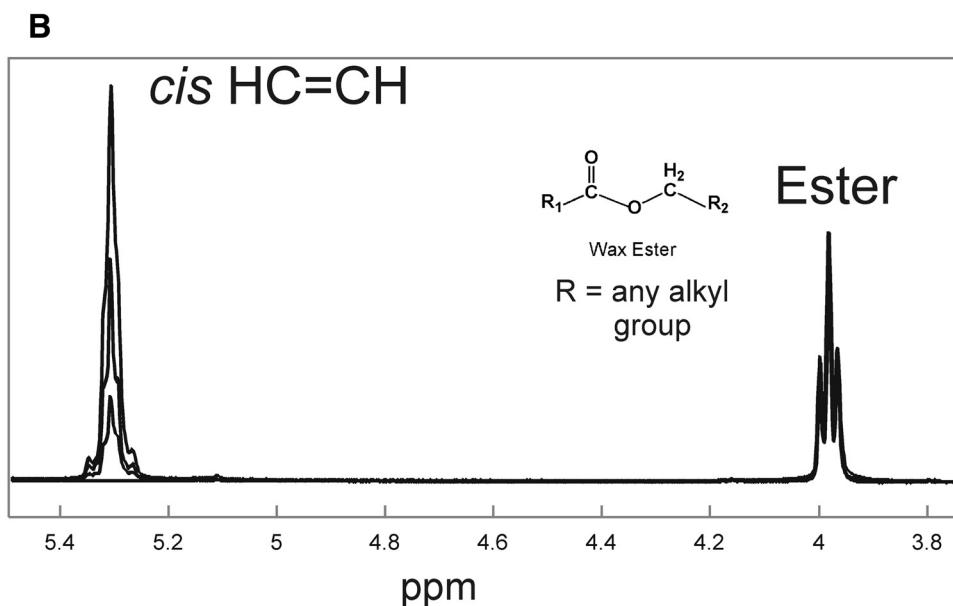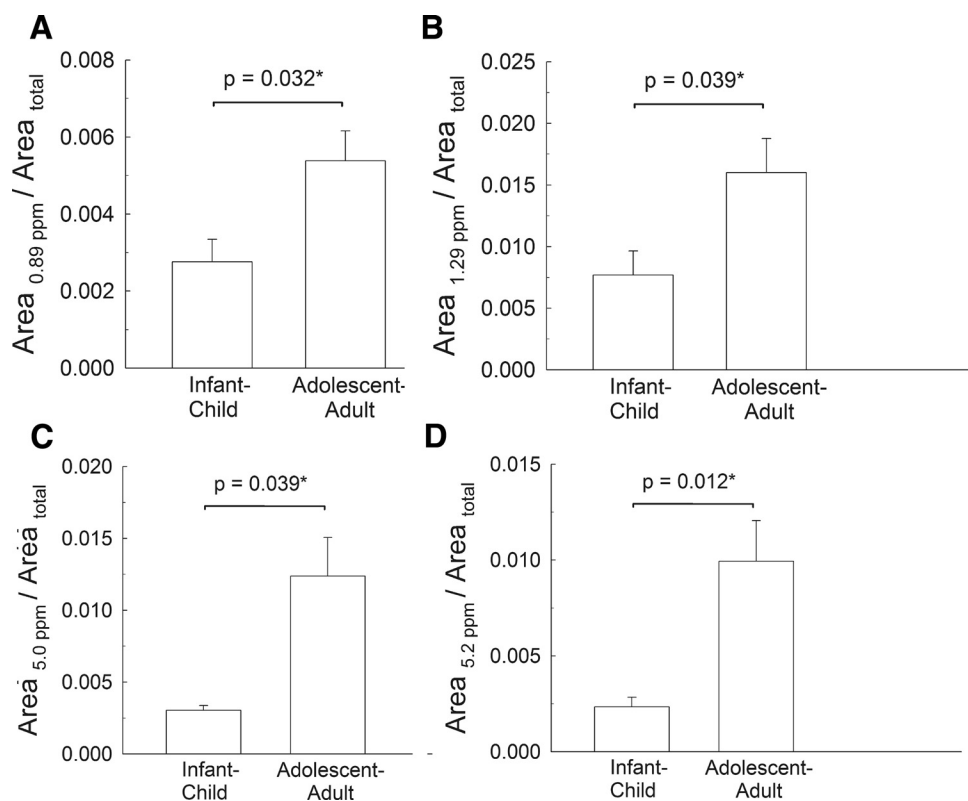
FIGURE 5. The relative areas of bands that change between the child group and adolescent-adult groups. Area total is the total area for all the resonances. Resonance assignments are given in Table 2. Sample data are provided in Table 1.

DISCUSSION

As discussed in the introduction, infants blink less often than adults without or with MGD. The tear break-up time is much longer in infants, 35 seconds compared to less than 5 seconds in adults with MGD. The amount of lipid on the lid margin increases with age and is lower in infants, so it is unlikely that the amount of lipid on the lid margin contributes to the stability of infant tears.[51] Furthermore, the amount of lipid on the lipid margin is not related to the instability of tears associated with MGD.[27] It is more likely that the quality of the meibum, rather than the quantity, is related to tear film stability.[27]

In this study we identified several proton resonances that change with age and could account for the decrease in tear film stability with age. With increasing age the relative amount of CH_3, $C=C$ bonds and degree of oxidation increase. The increase in CH_3 groups (Figs. 2A–C, 5A, 5B) and $C=C$ (Figs. 2E, 5C, 5D) with age was also observed by infrared spectroscopy.[22] The relative increase in CH_3 moieties with age is due to an increase in branching (Fig. 2B) and a decrease in the relative number of CH_2 protons (Fig. 2D).

The meibum content of lipid aldehydes and hydroperoxides increases with age (Fig. 6). ^{1}H NMR studies on the thermal oxidation of corn and sunflower oil show that, as oxidation

progresses, the relative amount of aldehydes relative to the amount of hydroperoxides increases.[49] We found that the aldehyde-to-hydroperoxide ratio increased with increasing age (Fig. 6), suggesting that the progression of oxidation was more advanced in the meibum of adolescents and adults compared with that in infants and children. The relationship between meibum lipid unsaturation and oxidation can be inferred from our studies of lens lipids. We found that unsaturated lipids in the human lens were more susceptible to oxidation than saturated ones.[52] Lens sphingolipids are three to four times more saturated than glycerolipids, and consequently they resist oxidation more effectively than unsaturated lipids.[53,54] Indeed, the rate constant for the propagation step of lipid oxidation decreases sharply when the number of lipid double bonds is reduced.[55] With sphingomyelin in the membrane, the degree and rate of oxidation of a polyunsaturated phosphatidylcholine were less than when a saturated phosphatidylcholine, rather than sphingomyelin, was present in the membrane,[56] thus suggesting that in addition to their high degree of saturation, sphingolipids form better interfacial barriers than glycerophospholipids.[56] From these lens studies, we can infer that because meibum from adults is more unsaturated, the lipids are more susceptible to lipid oxidation than is

TABLE 3. Integrated Relative Band Intensities of Resonances That Changed Significantly between the Child and Adolescent Groups

| Chemical Shifts (ppm)	Infant, Child Per Area of 1.39-ppm Resonance	Adolescent, Adult Per Area of 1.39-ppm Resonance	P^*	Infant, Child Per Area of 4.1-ppm Resonance	Adolescent, Adult Per Area of 4.1-ppm Resonance	P^*
0.89	0.010 ± 0.0021	0.0228 ± 0.0033	0.013	0.36 ± 0.08	1.66 ± 0.38	0.023
1.29	0.028 ± 0.0070	0.058 ± 0.01	0.039	0.95 ± 0.26	3.9 ± 0.71	0.004
5.0	0.011 ± 0.0012	0.05 ± 0.0097	0.005	0.35 ± 0.042	3.3 ± 0.81	0.011
5.2	0.0085 ± 0.0018	0.036 ± 0.0077	0.012	0.25 ± 0.030	2.7 ± 1.06	0.077

* Significant at $P < 0.05$.
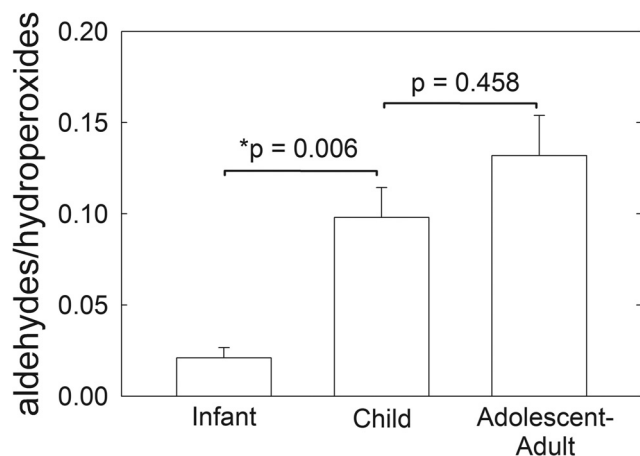
FIGURE 6. Two proton resonances related to aldehydes appear at 9.7 and 9.65 ppm. Two proton resonances related to hydroperoxides appear at 7.9 and 8.5 ppm. The areas of the two aldehyde resonances were divided by the areas of the two hydroperoxide resonances in the plot at the *top*. Sample data are provided in Table 1.

the more saturated infant meibum. This observation could explain why the degree of oxidation is higher in adult than in infant meibum.

An increase in branching or products of lipid oxidation such as aldehydes, hydroxyl, and hydroperoxyl moieties, especially toward the middle of the hydrocarbon chains would sterically hinder hydrocarbon chain lipid–lipid interactions because the lipids cannot pack close together to maximize van der Waal's interactions. *cis* C═C double bonds form kinks in hydrocarbon chains, and, similar to products of lipid oxidation and CH_3 branching, they hinder the packing of the hydrocarbon chains lowering van der Waal's interactions.[57] A decrease in lipid–lipid interactions with age has indeed been noted in an infrared spectroscopic study showing human meibum lipid order decreases from approximately 50% at 3 years of age to approximately 27% at 80 years of age.[22,28] Our studies on human age-related cataract[52] showed that lipid order increases with age[58] and even more with cataract.[59–61] The major factor governing the increase in order is hydrocarbon chain saturation,[21,23,52,62,63] which is believed to play a pivotal role in ordering waxes and human meibum with age.[21,23] The present ^{1}H NMR provides possible reasons for the decrease in meibum order with age and more *cis* C═C, aldehydes, hydroxyl, and hydroperoxyl moieties and CH_3 branching.

An infrared spectroscopic study also shows that with age, human meibum contains less protein,[20] and the lipid carbonyls are hydrogen bonded or in a more polar environment with age.[22] The amount of protein and the lipid order are related,[20] and it is possible that the loss of protein also contributes to the decrease in order with increasing age.

Do changes in meibum contribute to changes in tear film stability? Infants have much more stable tears than do adults. It is reasonable that tear film stability is higher in infants because their meibum contains less CH_3, C═C and aldehydes, relative to hydroperoxides, and are more ordered because of tighter and stronger lipid–lipid interactions and contain more protein. For water to evaporate, water molecules must first pass through the tight lipid–lipid barrier. For tears to break up, lipid–lipid interactions must be broken. It is reasonable that because the lipid–lipid interactions are stronger in infant tears, their tear film would be more stable and thus provide a better barrier to evaporation than would the tear film of adults. Lipid saturation could be the key property of meibum that stabilizes infant tears.

References

1. Mantelli F, Tiberi E, Micera A, Lambiase A, Visintini F, Bonini S. MUC5AC over expression in tear film of neonates. *Graefes Clin Exp Ophthalmol.* 2007;245:1377–1381.

2. Isenberg SJ, Del Signore M, Chen A, Wei J, Guillon J. The lipid layer and stability of the preocular tear film in newborns and infants. *Ophthalmology.* 2003;110:1408–1411.

3. Bacher LF. Factors regulating eye blink rate in young infants. *Optom Vis Sci.* 2010;87:337–343.

4. Lawrenson JG, Birhah R, Murphy PJ. Tear-film lipid layer morphology and corneal sensation in the development of blinking in neonates and infants. *J Anat.* 2005;206:265–270.

5. Sforza C, Rango M, Galante D, Bresolin N, Ferrario VF. Spontaneous blinking in healthy persons: an optoelectronic study of eyelid motion. *Ophthalmic Physiol Opt.* 2008;28:345–353.

6. Cho P, Yap M. Age, gender, and tear break-up time. *Optom Vis Sci.* 1993;70:828–831.

7. Mohidin N, Bay TC, Yap M. Non-invasive tear break-up time in normal Malays. *Clin Exp Optom.* 2002;85:37–41.

8. Ozdemir M, Temizdemir H. Age- and sex- related tear function changes in normal population. *Eye.* 2010;24:79–83.

9. Maïssa C, Guillon M. Tear film dynamics and lipid layer characteristics-effect of age and sex. *Contact Lens Anterior Eye.* 2010;33:176–182.

10. Sun WS, Baker RS, Chuke JC, Rouholiman BR. Age-related changes in human blinks. *Invest Ophthalmol Vis Sci.* 1997;38:92–99.

11. Lavezzo MM, Schellini SA, Padovani CR. Eye blink in newborn and preschool-age children. *Acta Ophthalmol.* 2008;86:275–278.

12. Craig J, Tomlinson A. Age and sex effects on the normal tear film. *Adv Exp Med Biol.* 1998;438:411–415.

13. Henderson JW, Prough WA. Influence of age, sex on flow of tears. *Arch Ophthalmol.* 1950;43:224–231.

14. Guillon M, Maïssa C. Tear film evaporation: effect of age and sex. *Cont Lens Anterior Eye.* 2010;33:171–175.

15. Cruz AA, Garcia DM, Pinto CT, Cehetti SP. Spontaneous eyeblink activity. *Ocul Surf.* 2011;9:29–41.

16. Foulks GN. The correlation between the tear film lipid layer and dry eye disease. *Surv Ophthalmol.* 2007;52:369–374.

17. Tsubota K, Hata S, Okusawa Y, Egami F, Ohtsuki T, Nakamori K. Quantitative videographic analysis of blinking in normal subjects and patients with dry eye. *Arch Ophthalmol.* 1996;114:715–720.

18. Tsubota K. Tear dynamics and dry eye. *Prog Retin Eye Res.* 1998;17:565–596.

19. Tomlinson A, Khanal S. Assessment of tear film dynamics: quantification approach. *Ocul Surf.* 2005;3:81–95.

20. Borchman D, Foulks GN, Yappert MC. Changes in human meibum lipid with meibomian gland dysfunction using principal component analysis. *Exp Eye Res.* 2010;91:246–256.

21. Oshima Y, Sato H, Zaghloul A, Foulks GN, Yappert MC, Borchman D. Characterization of human meibum lipid using Raman spectroscopy. *Curr Eye Res.* 2009;34:824–835.

22. Borchman D, Foulks GN, Yappert MC. Confirmation of changes in human meibum lipid infrared spectra with age using principal component analysis. *Curr Eye Res.* 2010;35:778–786.

23. Borchman D, Foulks GN, Yappert MC, et al. Human meibum lipid conformation and thermodynamic changes with meibomian-gland dysfunction. *Invest Ophthalmol Vis Sci.* 2011;52:3805–3817.

24. Borchman D, Foulks GN, Yappert MC, Tang D, Ho DV. Temperature-induced conformational changes in human tear lipids hydrocarbon chains. *Biopolymers Biospectrosc.* 2007;87:124–133.

25. Borchman D, Foulks GN, Yappert MC, Tang D, Ho DV. Spectroscopic evaluation of human tear lipids. *Chem Phys Lipids.* 2007;147:87–102.

26. Tiffany JM. Refractive index of meibomian and other lipids. *Curr Eye Res.* 1986;5:887–889.

27. Ashraf Z, Pasha U, Greenstone V, et al. Quantification of human sebum on skin and human meibum on the eye lid margin using sebum tape, spectroscopy and chemical analysis. *Curr Eye Res.* 2011;36:553–562.

28. Borchman D, Foulks GN, Yappert MC, et al. Physical changes in human meibum with age as measured by infrared spectroscopy. *Ophthalmic Res.* 2010;244:34–42.

29. Foulks GN, Borchman D, Yappert MC, Sung-Hye K, McKay JW. Topical azithromycin therapy of meibomian gland dysfunction: clinical response and lipid alterations. *Cornea.* 2010;29:781–788.

30. Foulks GN, Borchman D. Meibomian gland dysfunction: the past, the present, the future. *Eye Contact Lens.* 2010;36:249–253.

31. Huang L, Grami V, Marrero Y, et al. Human lens phospholipid changes with age and cataract. *Invest Ophthalmol Vis Sci.* 2005; 46:1682–1689.

32. Estrada R, Puppato A, Borchman D, Yappert MC. Re-evaluation of the phospholipid composition in membranes of adult human lenses by ^{31}-P NMR and MALDI-MS. *Biochim Biophys Acta.* 2010; 1798:303–311.

33. Ferguson-Yankey S, Borchman D, Taylor KG, DuPre DB, Yappert MC. Conformational studies of sphingolipids by NMR spectroscopy: I, dihydrosphingomyelin. *Biochim Biophys Acta.* 2000;1467:307–325.

34. Borchman D, Byrdwell WC, Yappert MC. Regional and age-dependent differences in the phospholipid composition of human lens membranes. *Invest Ophthalmol Vis Sci.* 1994;35:3938–3942.

35. Byrdwell WC, Borchman D, Porter RA, Taylor KG, Yappert MC. Separation and characterization of the unknown phospholipid in human lens membranes. *Invest Ophthalmol Vis Sci.* 1994;35: 4333–4343.

36. Merchant TE, Lass JH, Meneses P, Greiner JV, Glonek T. Human crystalline lens phospholipid analysis with age. *Invest Ophthalmol Vis Sci.* 1991;32:549–555.

37. Tulloch AP. Solvent effects on the nuclear magnetic resonance spectra of methyl hydroxysterates. *J Am Oil Chem Soc.* 1966;43: 670–674.

38. Verardo G, Pagani E, Geatti P. A thorough study of the surface wax of apple fruits. *Anal Biochem.* 2003;376:659–667.

39. Frost DJ, Barzilay J. Proton magnetic resonance identification of nonconjugated cis-unsaturated fatty acids and esters. *Anal Chem.* 1971;43:1316–1318.

40. Scano P, Marincola FC, Locci E, Lai A. ^{1}H and ^{13}C NMR studies of melon and head blubber of the striped dolphin (Stenella coeruleoalba). *Lipids.* 2006;41:1039–1048.

41. Tulloch AP. Beeswax: structure of the esters and their component hydroxyl acids and diols. *Chem Phys Lipids.* 1971;6:235–265.

42. Wineburg JP, Swern D. NMR chemical shift reagents in structural determination of lipid derivatives: II, methyl petroselinate and methyl oleate. *J Am Oil Chem Soc.* 1971;49:267–273.

43. KE PJ, Ackman RG. N.M.R. determination of wax esters in marine lipids. *Anal Chem Acta.* 1974;69:253–258.

44. Purcell JM, Morris SG, Susi H. Proton magnetic resonance spectra of unsaturated fatty acids. *Anal Chem.* 1966;38:588–592.

45. Johnson LF, Shoolery JN. Determination of unsaturation and average molecular weight of natural fats by nuclear magnetic resonance. *Anal Chem.* 1962;34:1136–1139.

46. Glass CA, Dutton HJ. Determination of beta-olefinic methyl groups in esters of fatty acids by nuclear magnetic resonance. *Anal Chem.* 1964;36:2401–2404.

47. Robosky LC, Wade K, Woolson D, et al. Quantitative evaluation of sebum lipid components with nuclear magnetic resonance. *J Lipid Res.* 2008;49:686–692.

48. Shrestha RK, Borchman D, Foulks GN, Yappert MC. Analysis of the composition of lipid in human meibum from normal infants, children, adolescents, adults and adults with meibomian gland dysfunction using ^{1}H-NMR spectroscopy. *Invest Ophthalmol Vis Sci.* 2011;52:7350–7358.

49. Guillén MD, Ruiz A. Oxidation process of oils with high content of linoleic acyl groups and formation of toxic hydroperoxy- and hydroxyalkenals: a study by ^{1}H nuclear magnetic resonance. *J Sci Food Agric.* 2005;85:2413–2420.

50. Haywood RM, Claxson AW, Hawkes GE, et al. Detection of aldehydes and their conjugated hydroperoxydiene precursors in thermally-stressed culinary oils and fats: investigations using high resolution proton NMR spectroscopy. *Free Radic Res.* 1995;22:441–482.

51. Chew CKS, Hykin PG, Jansweijer C, Dikstein S, Bron AJ. The casual level of meibomian lipids in humans. *Curr Eye Res.* 1993;12:255–259.

52. Borchman D, Yappert MC. Lipids and the ocular lens. *J Lipid Res.* 2010;51:2473–2488.

53. Byrdwell CW, Borchman D. Liquid chromatography/mass spectrometric characterization of the unknown phospholipid of human lens membranes. *Ophthalmic Res.* 1997;29:191–206.

54. Deeley JM, Mitchell TW, Wei X, et al. Human lens lipids differ markedly from those of commonly used experimental animals. *Biochim Biophys Acta.* 2008;1781:288–298.

55. Witting LA. Lipid peroxidation in vivo. *J Am Oil Chem Soc.* 1965; 42:908–913.

56. Oborina EM, Yappert MC. Effect of sphingomyelin versus dipalmitoylphosphatidylcholine on the extent of lipid oxidation. *Chem Phys Lipids.* 2003;123:223–232.

57. Lamba OP, Lal S, Yappert MC, Borchman D. Spectroscopic detection of lipid peroxidation products and structural changes in a sphingomyelin model system. *Biochem Biophys Acta.* 1991;1081: 181–187.

58. Borchman D, Ozaki Y, Lamba OP, Byrdwell WC, Yappert MC. Age and regional structural characterization of clear human lens lipid membranes by infrared and near-infrared Raman spectroscopies. *Biospectroscopy.* 1996;2:113–123.

59. Borchman D, Lamba OP, Yappert MC. Structural characterization of lipid membranes from clear and cataractous human lenses. *Exp Eye Res.* 1993;57:199–208.

60. Paterson CA, Zeng J, Husseini Z, et al. Calcium ATPase activity and membrane structure in clear and cataractous human lenses. *Curr Eye Res.* 1997;16:333–338.

61. Huang L, Grami V, Marrero Y, et al. Human lens phospholipid changes with age and cataract. *Invest Ophthalmol Vis Sci.* 2005; 46:1682–1689.

62. Borchman D, Tang D, Yappert MC. Lipid composition, membrane structure relationships in lens and muscle sarcoplasmic reticulum membranes. *Biospectroscopy.* 1999;5:151–167.

63. Borchman D, Giblin FJ, Yappert MC, et al. Impact of aging and hyperbaric oxygen in vivo on guinea pig lens lipid and nuclear light scatter. *Invest Ophthalmol Vis Sci.* 2000;41:3061–3073.